High Curie temperature and carrier mobility of novel Fe, Co and Ni carbide MXenes

Y. Hu, [1] X. Y. Liu, [2] Z. H. Shen,[1] Z. F. Luo ,[1] Z. G. Chen,[1] X. L. Fan [1]*

[1] State Key Laboratory of Solidification Processing, Center for advanced lubrication and seal Materials, School of Material Science and Engineering, Northwestern Polytechnical University, 127 YouYi Western Road, Xi'an, Shaanxi 710072, China

[2] Queen Mary University of London Engineering School, Northwestern Polytechnical University, 127 YouYi Western Road, Xi'an, Shaanxi 710072, China

*xlfan@nwpu.edu.cn

Calculation of the high-order three-spin coupling parameters

The spin Hamiltonian including the Heisenberg exchange terms and the three-spin interactions is written as

$$H = -\sum_{i,j} J_1 M_i M_j - \sum_{k,l} J_2 M_k M_l - \sum_{i,i',j} J_1'(M_i M_j)(M_j M_{i'}) - \sum_{k,k',l} J_2'(M_k M_l)(M_l M_{k'})$$

where J_1, J_2 are the nearest neighboring (NN), second NN exchange constants, J_1' and J_2' are the interlayer and intralayer three-spin coupling parameters. J_1, J_2, J_1' and J_2' are calculated via the energy difference between the FM and AFM states shown in Fig. S10 as.

$$J_1 = \frac{E_{AFM1} - E_{FM}}{24M^2}$$

$$J_2 = \frac{E_{AFM4} - E_{AFM3}}{-8M^2}$$

$$J_1 - 2J_2'M^2 = \frac{E_{AFM3} - E_{AFM2}}{8M^2}$$

$$\frac{1}{4}J_1 + J_2 + \frac{1}{4}J_1'M^2 + J_2'M^2 = \frac{E_{AFM2} - E_{FM}}{32M^2}$$

Table S1. The calculated elements of 2D elastic constants matrix and the in-plane stiffness for MXenes M_2C and M_2CT_2 (M= Fe, Co, Ni; T=F, O, OH).

	C_{11} ($J \cdot m^{-2}$)	C_{22} ($J \cdot m^{-2}$)	C_{66} ($J \cdot m^{-2}$)	C_{12} ($J \cdot m^{-2}$)	C_{21} ($J \cdot m^{-2}$)	E_x ($J \cdot m^{-2}$)	E_y ($J \cdot m^{-2}$)
Fe_2C	52.61	52.61	23.05	6.51	6.51	51.80	51.80
Co_2C	72.50	72.50	38.61	-4.72	-4.72	72.19	72.19
Ni_2C	77.70	77.70	35.96	5.77	5.77	77.27	77.27
Fe_2CF_2	150.67	150.67	46.50	57.68	57.68	128.59	128.59
Fe_2CO_2	221.16	221.16	75.18	70.81	70.81	198.49	198.49
$Fe_2C(OH)_2$	203.58	203.58	68.30	66.99	66.99	181.54	181.54
Co_2CF_2	172.90	172.90	63.85	45.21	45.21	161.08	161.08
Co_2CO_2	192.80	192.80	61.90	69.00	69.00	168.11	168.11
$Co_2C(OH)_2$	205.32	205.32	60.49	84.34	84.34	170.67	170.67
Ni_2CF_2	154.68	154.68	45.50	63.68	63.68	128.46	128.40
Ni_2CO_2	106.47	106.47	44.93	16.62	16.62	103.88	103.88
$Ni_2C(OH)_2$	62.69	62.69	45.38	-28.07	-28.07	50.12	50.12

Table S2. The calculated lattice constants (a1 and a2), distances between the M atoms and its nearest neighboring C atoms (M-C), and T groups (M-T), distance between nearest neighboring (NN), second NN and third NN magnetic coupling pairs (d_1, d_2 and d_3), the formation energies ($E_{\text{form-M}_2\text{C}}$) for M_2C and adsorption energies of T-groups ($E_{adsor-T}$) for M_2CT_2.

	Fe_2C	Co_2C	Ni_2C	Fe_2CF_2	Fe_2CO_2	$Fe_2C(OH)_2$	Co_2CF_2	$Co_2C(OH)_2$	Ni_2CF_2
a1=a2 (Å)	2.84	2.93	2.94	2.93	2.83	2.87	2.94	2.96	2.93
M-C (Å)	1.92	1.90	1.91	1.94	2.02	1.92	1.84	1.85	1.97
M-T(Å)	-	-	-	1.97	1.94/1.93*	2.06	1.94	1.98	2.07
d_1 (Å)	2.00	2.42	-	2.57	2.59	2.62	-	-	-
d_2 (Å)	2.84	2.93	-	2.93	2.83	2.87	-	-	-
d_3 (Å)	3.84	3.80	-	3.92	3.94	3.94	-	-	-
$E_{\text{form-M}_2\text{C}}$ rich condition	-0.38	-0.34	-0.47	-	-	-	-	-	-
(eV/atom) poor condition	-2.41	-2.45	-2.54	-	-	-	-	-	-
$E_{\text{adsor-T}}$ (eV/atom)	-	-	-	-1.276	-0.669	-1.423	-1.145	-1.412	-1.049

* distance between the M atoms and its nearest neighboring T atoms locating on the B sites.

Table S3. The calculated nearest neighboring (NN), second NN and third NN magnetic coupling parameters (J_1, J_2 and J_3) at the HSE06 level, Curie temperature/Neel temperature ($T_{C/N}^{MC}$) for Fe_2C, Co_2C, Fe_2CF_2, Fe_2CO_2 and $Fe_2C(OH)_2$.

	Fe_2C	Co_2C	Fe_2CF_2	Fe_2CO_2	$Fe_2C(OH)_2$
J_1 (meV)	6.07	14.22	21.38	26.35	3.78
J_2 (meV)	5.82	3.87	5.71	-16.83	2.93
J_3 (meV)	0.25	0.26	0.23	-0.88	0.32
$T_{C/N}^{MC}$ (K)	590	170	920	40	290

Table S4. The calculated nearest neighboring (NN), second NN exchange constantes, as well as the interlayer and intralayer three-spin coupling constants (J_1, J_2, J_1' and J_2') at the HSE06 level, Curie temperature/Neel temperature ($T_{C/N}^{MC}$) based on the extended Heisenberg model for Fe_2C, Co_2C, Fe_2CF_2, Fe_2CO_2 and $Fe_2C(OH)_2$.

	Fe_2C	Co_2C	Fe_2CF_2	Fe_2CO_2	$Fe_2C(OH)_2$
J_1 (meV)	6.32	14.48	21.61	25.47	4.10
J_2 (meV)	4.86	2.27	4.12	-16.73	2.37
J_1' (meV)	0.59	4.84	1.25	4.88	0.08
J_2' (meV)	0.13	0.52	0.12	-1.76	0.16
$T_{C/N}^{MC}$ (K)	570	150	880	40	270

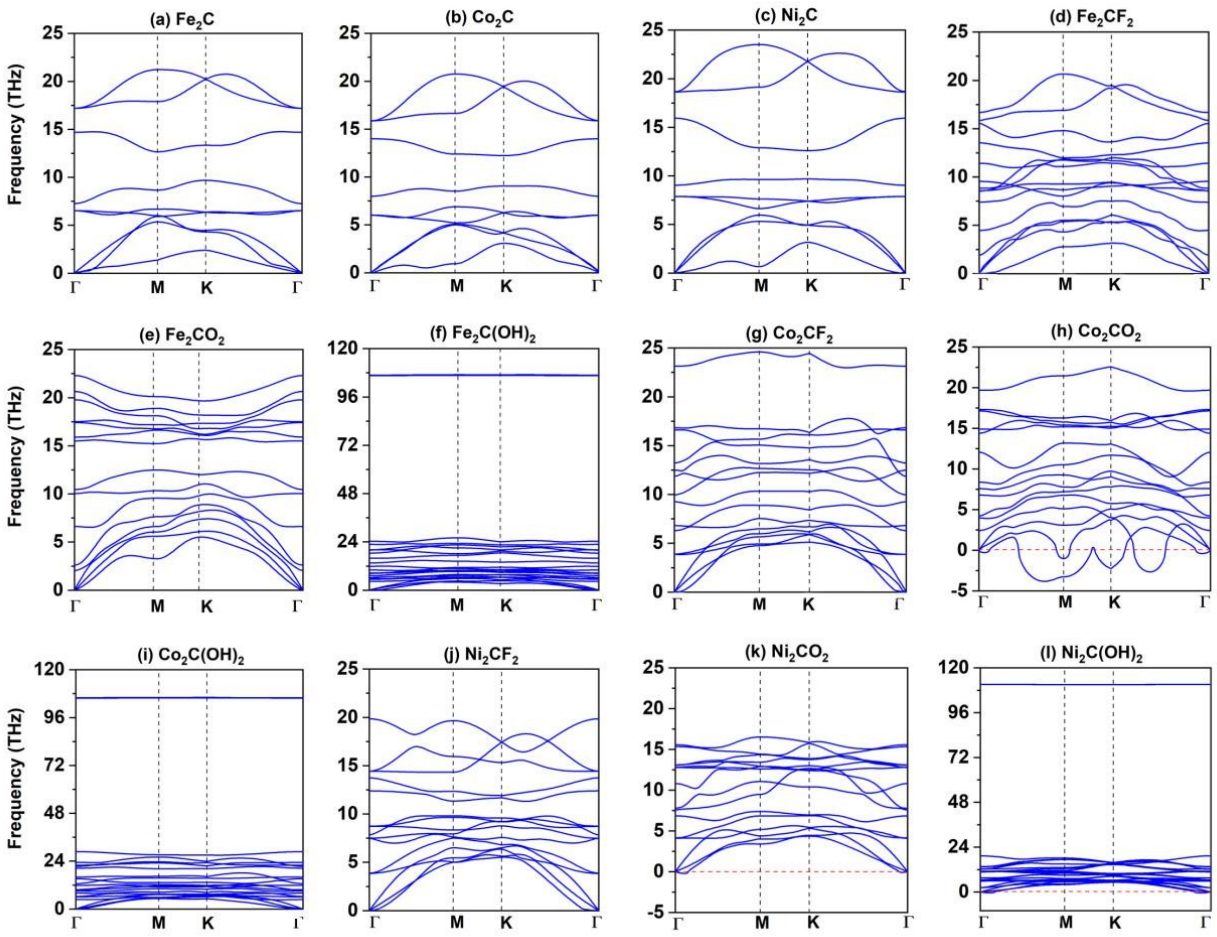

Fig. S1. The phonon spectrums for MXenes M_2C and M_2CT_2 (M= Fe, Co, Ni; T= F, O, OH).

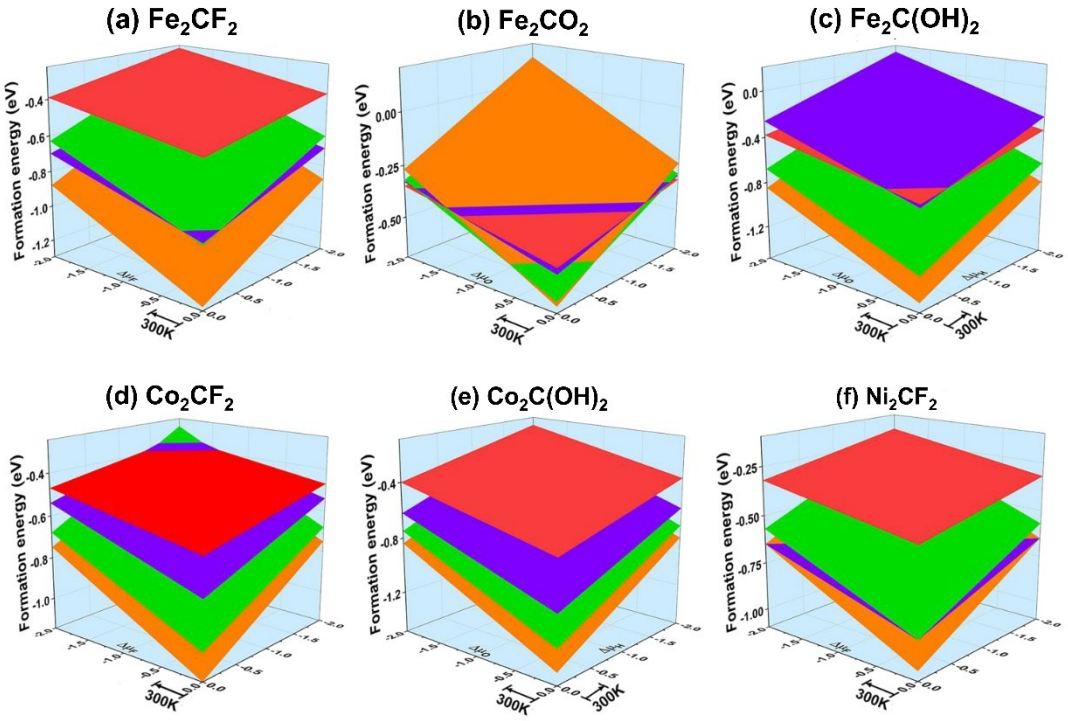

Fig. S2. Adsorption energies of terminal groups T (F, O, OH) for Fe_2CF_2, Fe_2CO_2, $Fe_2C(OH)_2$, Co_2CF_2, $Co_2C(OH)_2$ and Ni_2CF_2 at 25% (red), 50% (purple), 75% (green) and 100% (orange) coverage as a function of $\Delta\mu = \mu - (1/2)E(T_2)$, μ is the chemical potential of F, O and H, $E(T_2)$ is the energy of T_2 molecule in gas phase for T being F, O and H.

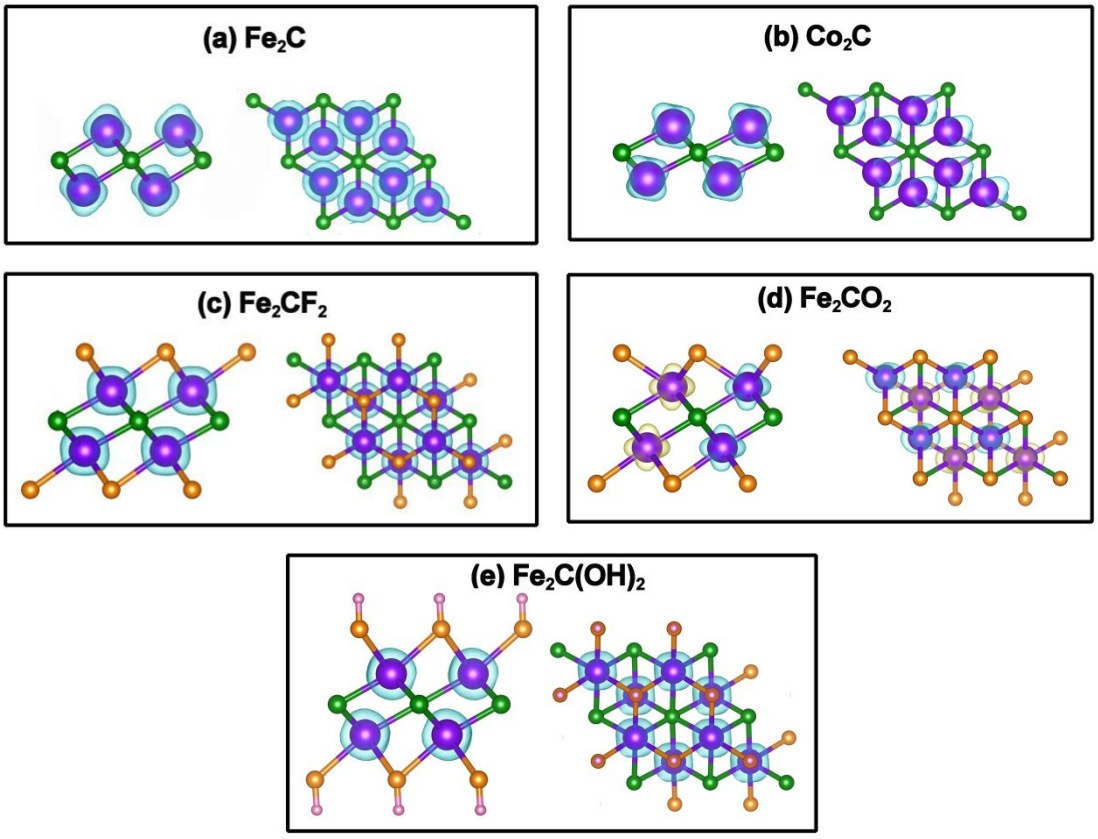

Fig. S3. Side and top views of spin-resolved charge densities (SCD) for (a) Fe_2C, (b) Co_2C, (c) Fe_2CF_2, (d) Fe_2CO_2 and (e) $Fe_2C(OH)_2$. Blue and orange areas represent positive and negative SCD. The isosurface value is 0.02 $eÅ^{-3}$.

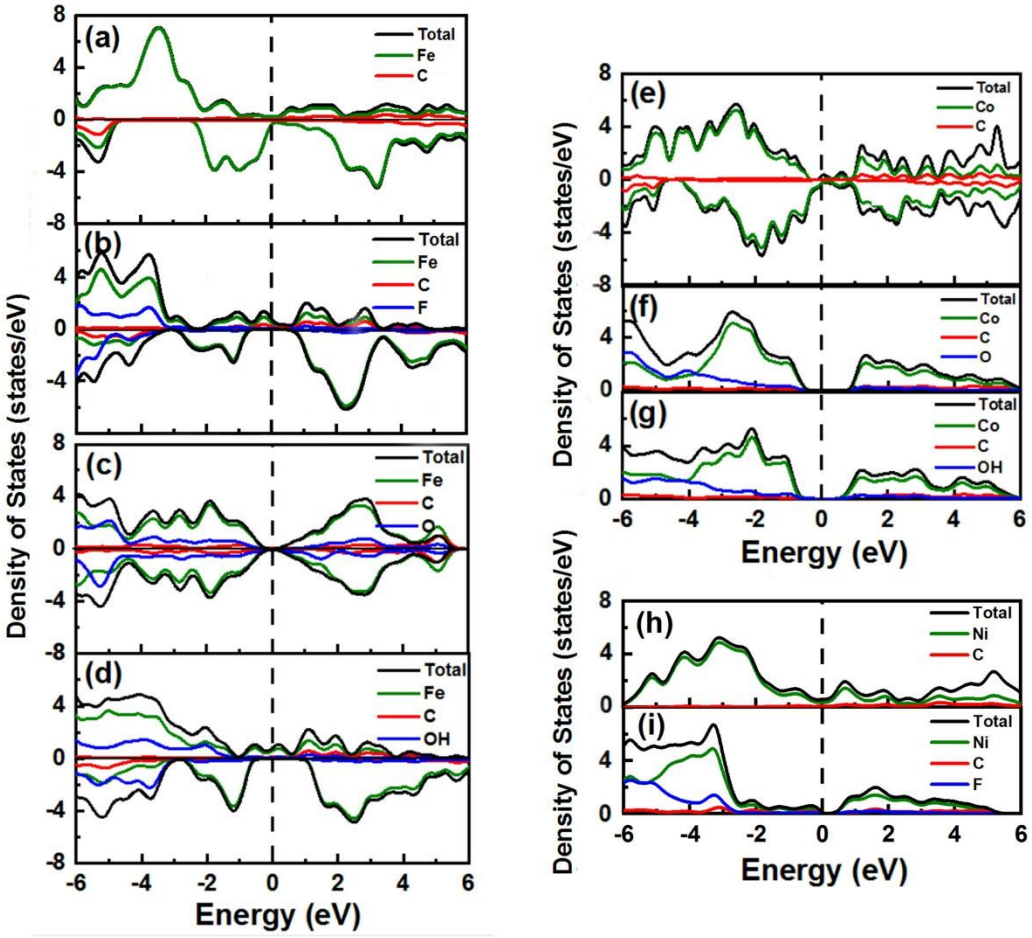

Fig. S4. Density of states for (a) Fe_2C, (b) Fe_2CF_2, (c) Fe_2CO_2, (d) $Fe_2C(OH)_2$, (e) Co_2C, (f) Co_2CF_2, (g) $Co_2C(OH)_2$, (h) Ni_2C and (i) Ni_2CF_2. The Fermi level is set as 0 eV.

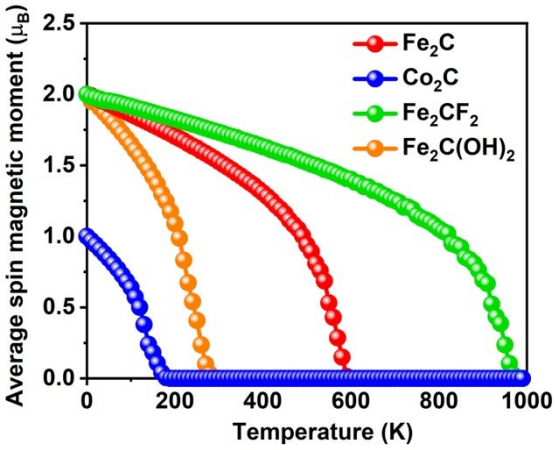

Fig. S5. On-site magnetic moments of M atoms as a function of temperature for ferromagnetic MXenes Fe_2C, Co_2C, Fe_2CF_2 and $Fe_2C(OH)_2$.

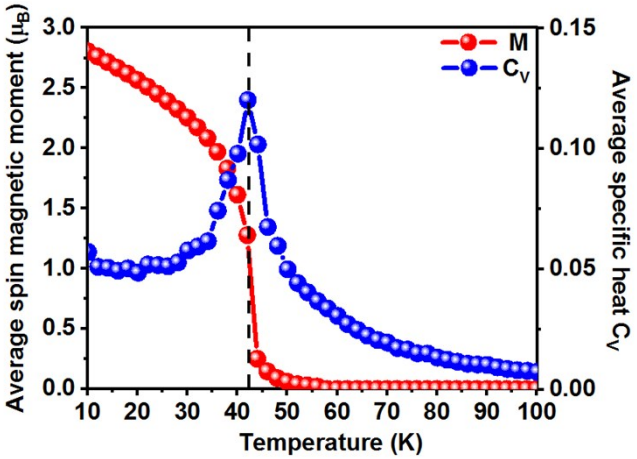

Fig. S6. Average specific heat and on-site magnetic moments of Cr atoms as a function of temperature for CrI_3 monolayer, the value of J and A are obtained from Ref. S1.

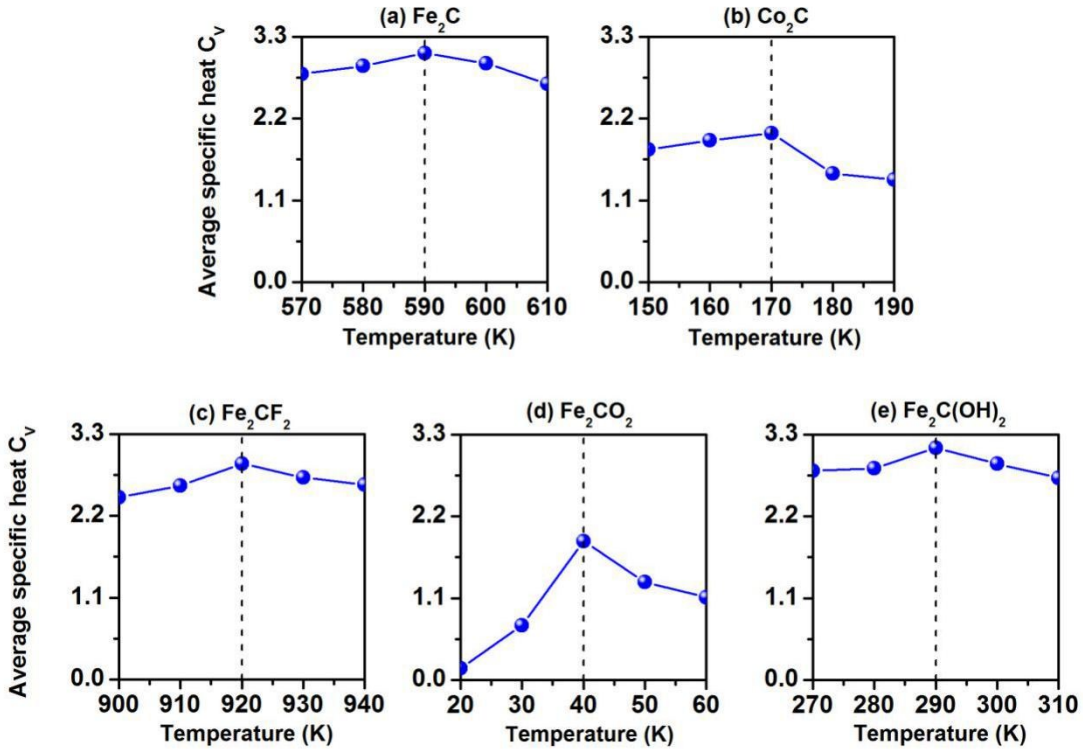

Fig. S7. Average specific heat for ferromagnetic (a) Fe_2C, (b) Co_2C, (c) Fe_2CF_2, (e) $Fe_2C(OH)_2$, and (d) anti-ferromagnetic Fe_2CO_2 as functions of temperature. The magnetic coupling parametres (J_1, J_2 and J_3) were obtained by adopting the HSE06 method.

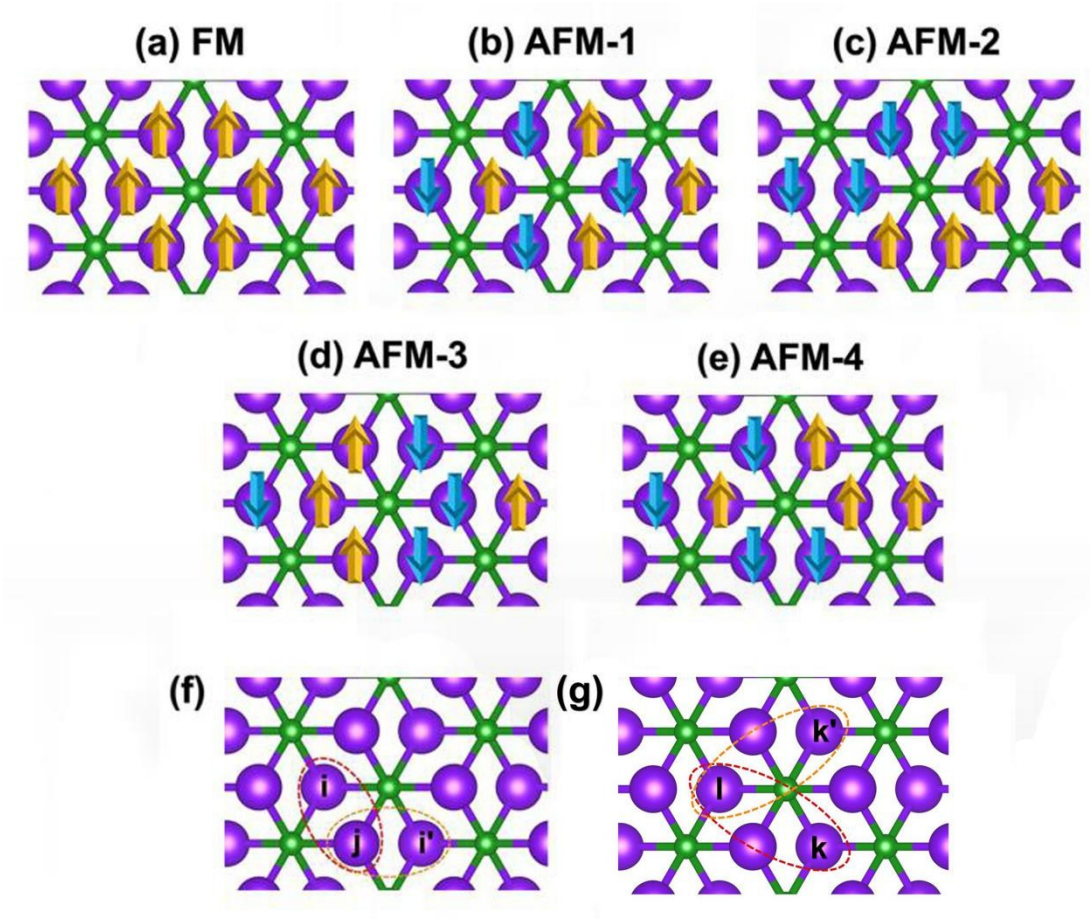

Fig. S8. Schematic diagrams for MXenes M_2C and M_2CT_2 (M= Fe, Co, Ni; T= F, O, OH) in (a) ferromagnetic (FM), (b) anti-ferromagnetic (AFM-1), (c) AFM-2, (d) AFM-3 and (e) AFM-4 states in $2\times2\times1$ supercell, (f) and (g) shows the three-spin interactions. The yellow and blue arrows represent spin-up and spin-down states of M atoms, respectively.

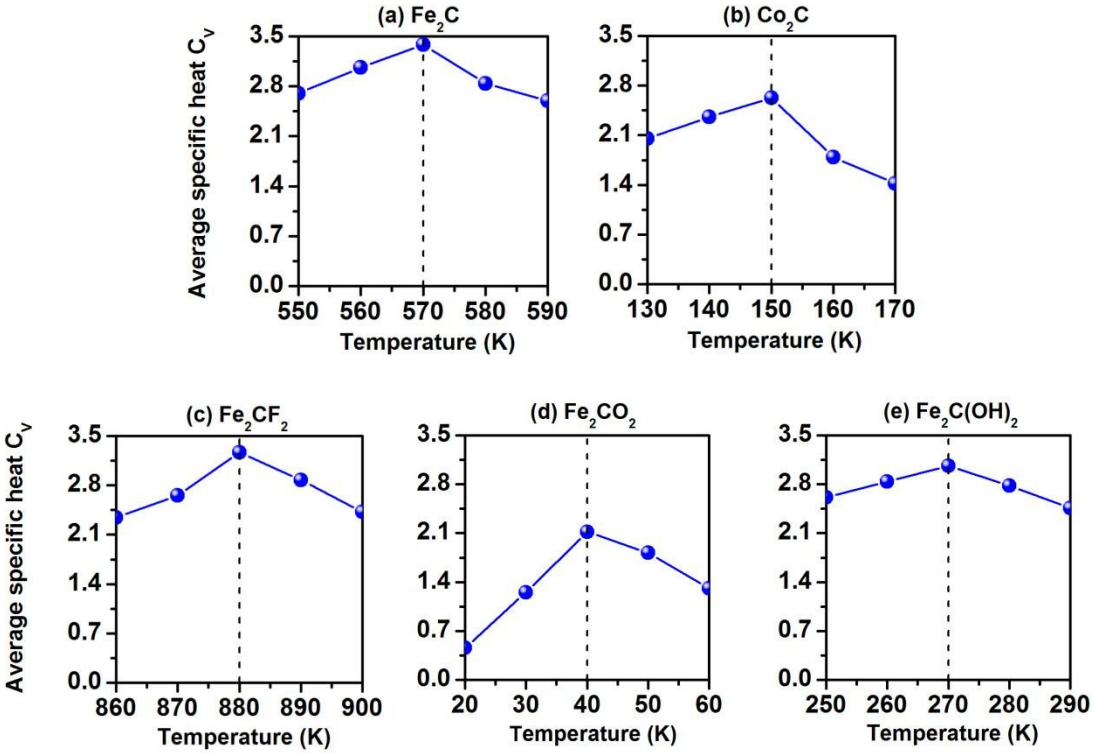

Fig. S9. Average specific heat for ferromagnetic (a) Fe_2C, (b) Co_2C, (c) Fe_2CF_2, (e) $Fe_2C(OH)_2$, and (d) anti-ferromagnetic Fe_2CO_2 as functions of temperature based on extended Heisenberg model with considering the three-spin interactions at HSE06 level.

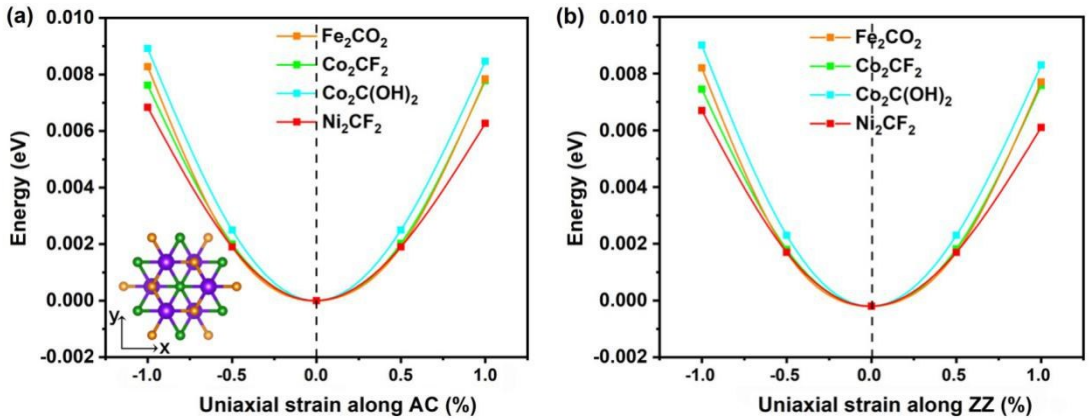

Fig. S10. Changes of total energies for semiconducting MXenes Fe_2CO_2, Co_2CF_2, $Co_2C(OH)_2$ and Ni_2CF_2 with respect to uniaxial strain along (a) armchair (AC) and (b) ziazag (ZZ) directions.

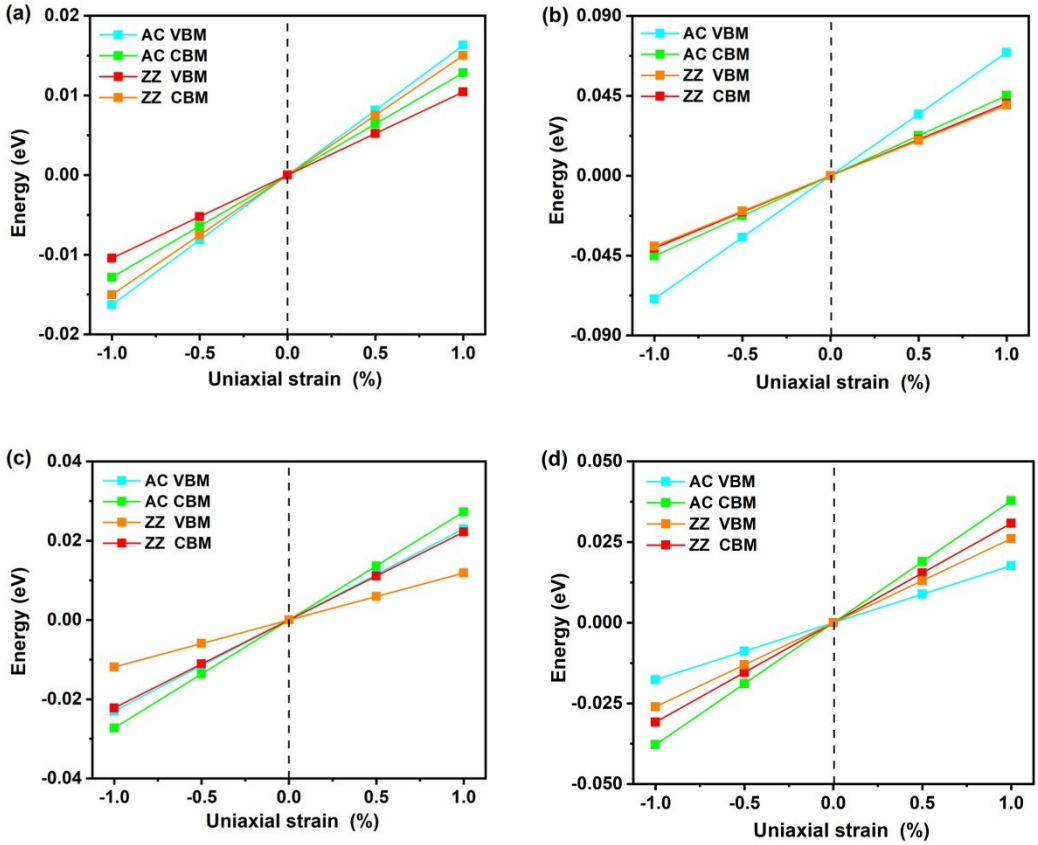

Fig. S11. Shift of valence band maximum (VBM) and conduction band minimum (CBM) with respect to uniaxial strain along the armchair (AC) and ziazag (ZZ) directions for semiconducting MXenes (a) Fe_2CO_2, (b) Co_2CF_2, (c) $Co_2C(OH)_2$ and (d) Ni_2CF_2.

References

1. W. B. Zhang, Q. Qu, P. Zhu, and C. H. Lam, *J. Mater. Chem. C*, 2015, **3,** 12457.